Washington Photometry of the Globular Cluster System of NGC 4472. II. The Luminosity Function and Spatial Structure

Myung Gyoon Lee[1], Eunhyeuk Kim
Department of Astronomy, Seoul National University, Seoul 151-742, Korea
Electronic mail: mglee@astrog.snu.ac.kr, ekim@astro.snu.ac.kr

and

Doug Geisler[1]
KPNO/NOAO, Tucson, AZ 85719, USA
Electronic mail: dgeisler@noao.edu

ABSTRACT

We present a comprehensive study of the luminosity function and spatial structure of the globular cluster system of NGC 4472, the brightest galaxy in Virgo, based on deep wide field Washington CT_1 CCD images. The globular cluster luminosity function shows a peak at $T_1 = 23.3 \pm 0.1$ mag, about 1.5 mags brighter than our 50% completeness limit. Comparing this value with that of the Galactic globular clusters, we estimate the true distance modulus to NGC 4472 to be $(m-M)_0 = 31.2 \pm 0.2$ (corresponding to a distance of 17.4 ± 1.6 Mpc). With our large sample (≈ 2000) of bright globular clusters over a wide field, we make a definitive investigation of the spatial structures of the metal-poor and metal-rich cluster populations and find that they are systematically different: (1) The metal-rich clusters are more centrally concentrated than the metal-poor clusters; and (2) The metal-rich clusters are elongated roughly along the major axis of the parent galaxy, while the metal-poor clusters are essentially spherically distributed. In general, the metal-rich clusters closely follow the underlying halo starlight of NGC 4472 in terms of spatial structure and metallicity, while the metal-poor clusters do not. The global value of the specific frequency of the globular clusters in NGC 4472 is estimated to be $S_N = 4.7 \pm 0.6$. The local specific frequency increases linearly outward from the center of NGC 4472 until $\sim 5'.5$, beyond which it levels off at $S_N \sim 8.5$ until the limit of our data at $7'$. The specific frequency of both the metal-rich and metal-poor populations shows similar behavior. However, S_N of the metal-poor clusters is about a factor 2 larger than that of the metal-rich clusters in the outer regions. Implications of these results for the origin of the globular clusters in NGC 4472 are discussed. These results are consistent with many of the predictions of both the model of episodic *in situ* formation plus tidal stripping of globular clusters given by Forbes *et al.* [1997, AJ, 113, 1652] and the Ashman & Zepf [1992, ApJ, 384, 50] merger formation model, but each of the models also has some problems.

1. INTRODUCTION

This is the second in a series of papers on Washington CCD photometry of the globular cluster system (GCS) in NGC 4472. In Paper I (Geisler *et al.* 1996) we obtained a deep color-magnitude diagram of

[1]Visiting Astronomer, Kitt Peak National Observatory, National Optical Astronomy Observatories, operated by the Association of Universities for Research in Astronomy, Inc., under contract with the National Science Foundation.

≈10,000 objects in a $16'.4 \times 16'.4$ field centered on NGC 4472, and presented the analysis of the metallicities of about 1800 bright ($T_1 < 23$ mag) globular clusters. Our most striking result was that the metallicity distribution of the globular clusters was clearly bimodal, showing distinct peaks at [Fe/H] = –1.3 and –0.1 dex.

In this paper we examine the globular cluster luminosity function (GCLF) and spatial structure of the NGC 4472 GCS. This study is based on data for a large number of globular cluster candidates in NGC 4472 obtained from deep wide field CCD photometry, while previous studies on this subject were based either on shallow wide field photographic photometry or on deep small field CCD photometry (Harris & Petrie 1978, Harris & van den Bergh 1981, Harris 1986, Cohen 1988, Harris *et al.* 1991, Couture *et al.* 1991).

The use of the turnover of the GCLF has become increasingly important as a distance indicator. Jacoby *et al.* (1992) have shown that this technique is more precise than previously regarded. The peak of the GCLF in several Virgo galaxies has been used to derive their distances (e.g. Harris *et al.* 1991, Whitmore *et al.* 1995, Elson & Santiago 1996). Our large sample should allow us to obtain a more robust value than derived from previous smaller-scale studies. Secondly, Ashman *et al.* (1995) have predicted a metallicity dependence of the GCLF peak, with metal-poor clusters peaking at brighter magnitude than metal-rich clusters, with the exact values depending on the metallicity and bandpass. Whitmore *et al.* (1995)'s HST data on the M87 GCS showed a bimodal metallicity distribution and the GCLFs of the two populations showed peaks which differed by about the amount predicted by Ashman *et al.* . The presence of another bimodal GCS allows another critical test of the Ashman *et al.* prediction, as cluster populations with significantly different metallicities can be compared directly.

The utility of a global measure of the globular cluster population in a galaxy, namely the specific frequency S_N, has been shown by many studies (e.g. Harris 1991). This provides a luminosity-independent means of comparing the cluster formation efficiencies of different galaxies, a key ingredient in understanding how the clusters and the galaxies themselves are made. Likewise, the spatial structure of the GCS and how it compares to the galaxy light has been used since the seminal study of Strom *et al.* (1981) to set constraints on the relative formation and chemical evolution histories of these components. The presence of two distinct GC populations in NGC 4472 allow us to investigate their specific frequencies and spatial structures independently. Such investigations are unprecedented. Note that HST studies are generally confined to only a very small inner region of the GCS, while wide-field ground-based studies such as ours cover virtually the entire extent of the GCS **except** for the inner regions, which are saturated and/or subject to crowding and high background light levels. Thus, HST and ground-based studies are very complementary.

This paper is organized as follows. Section 2 describes briefly the data for the globular clusters used in this study. Sec. 3 derives the GCLF and estimates the distance to NGC 4472. Sec. 4 estimates the specific frequency of the GCS in NGC 4472 and investigates its variation with galactocentric radius. Sec. 5 studies the spatial structure of the GCS and compares this with the structure of the underlying halo starlight of NGC 4472. Sec. 6 summarizes our results and compares them with the predictions of various models of the formation of globular clusters in giant elliptical galaxies. Preliminary results of this study were presented in several conference proceedings (Lee *et al.* 1996, Kim *et al.* 1996).

2. THE DATA

We have used the photometric data of the objects in a $16'.4 \times 16'.4$ field centered on NGC 4472 given in Paper I. The KPNO 4m PF/CCD system was used to obtain deep Washington system (Canterna 1976) CT_1 observations, and the data were reduced with the DAOPHOT II psf-fitting reduction program. Figure 1 displays the color-magnitude diagram of the ≈10,000 measured objects. The remarkable bimodal vertical structure graphically portrays the two populations of globular clusters in NGC 4472, and the faint blue horizontal structure represents mostly background galaxies, as described in detail in Paper I. Here, we have chosen, as the best globular cluster candidates, those objects with colors of $1.0 < (C - T_1) < 2.3$ for investigating the GCLF, going down to our incompleteness limit of $T_1 = 24.6$ (see below), and have used the bright globular clusters, with $19.63 < T_1 < 23$ mag for the analysis of the spatial structure of the GCS, as marked in Figure 1. These limits (other than the completeness limit determined below) were derived in Paper I from a careful analysis of the color, magnitude and spatial distribution of our entire sample of objects. We have relaxed the photometric error requirement for this analysis to $\sigma(C - T_1) < 0.15$. This increases our final sample of GC candidates to ~ 2000.

Since the color distribution of the globular clusters in NGC 4472 is clearly bimodal with a minimum at $(C - T_1) \sim 1.65$, and an age difference sufficiently large to explain the observed color difference is very unlikely (Paper I), we assume the colors reflect metallicity and have divided the final sample into two groups accordingly: the blue globular clusters ($1.0 < (C - T_1) < 1.65$, 1257 objects) and the red globular clusters ($1.65 < (C - T_1) < 2.3$, 764 objects) (see Paper I). The mean metallicities of each of these two groups are, respectively, [Fe/H] = –1.3 dex and –0.1 dex. These two groups are referred to as BGCs (blue or metal-poor GCs) and RGCs (red or metal-rich GCs), respectively, hereafter. The number ratio of the metal-rich GCs to metal-poor GCs is 0.6. Inspection of the color-magnitude diagram and luminosity function in the next section indicates that the contamination due to background galaxies and foreground stars is minor (less than 10 %) in the final sample of the bright globular clusters with $T_1 < 23$ mag (see also Paper I).

3. THE GLOBULAR CLUSTER LUMINOSITY FUNCTION

3.1. Completeness Tests

We have tested the completeness of our photometry using artificial star experiments with the aid of the ADDSTAR routine in DAOPHOT II. We have added 20,000 artificial stars into 10 copies of the original images (2,000 stars per image), and have estimated the completeness of our photometry by calculating the recovery probability of the added stars. Table 1 lists the completeness as a function of magnitude. The completeness in Table 1 is defined as $f(C, T_1)$ = N(recovered stars) / N(added stars).

The incompleteness varies depending on position in the image, and is especially large in the central region because of the saturation due to the bright nucleus of NGC 4472, and in the outer region due to image quality degradation from the large, poorly corrected 4m PF/CCD field. Therefore we have limited our final sample to the globular clusters located within the galactocentric radius range of $50'' < r < 420''$ for the following analysis. The lower limit has been increased over that used in Paper I to ensure uniform completeness over the range.

Table 1 shows that our photometry is almost complete up to $T_1 \sim 24$ mag and $C \sim 25$ mag, and the limiting magnitude, defined as the 50% completeness level, is $T_{1,lim} \sim 24.6$ mag and $C_{lim} \sim 25.9$ mag. Table 1 also lists the mean differences of the magnitudes of the added and recovered stars, which shows

this quantity is generally small until one approaches the limiting magnitude. We also include the mean photometric errors (the rms of the differences). These values agree well with the internal errors returned by DAOPHOT.

3.2. The Globular Cluster Luminosity Function

We have derived the luminosity function of this sample and the results are shown in Figure 2 and listed in Table 2a. Before discussing these results, we must first note the limitations of our data. The area covered by this sample is only 152 square arcmin, although the CCD field covered 269 square arcmin and reaches $r > 8'$ from the center of the galaxy. Unfortunately, we have had to limit our sample to this smaller radial range because of the increasingly poor image quality beyond this. Therefore, we are only able to study the GCS from $\sim 1' - 7'$. Indeed, due to this same problem, we are unable to derive any measure of the background contamination since we are unable to perform useful photometry in a region far enough from the galaxy to lie beyond the extent of the GCS (note that Harris 1986 estimates the GCs to extend out to $r \sim 20'$) despite our efforts to do so. We were also unable to observe a separate comparison field due to time constraints. In addition, the strongly varying image quality prohibited us from performing the usual image classification analysis. We attempted to use the various image moments defined by Harris *et al.* (1991) to differentiate GCs from resolved background galaxies, but our attempts proved unsatisfactory. Therefore we could not discard resolved objects from our analysis or subtract the contribution due to field populations from the derived luminosity function of the globular clusters. Instead we have investigated roughly the contamination effect on the resulting luminosity function of the globular cluster candidates as follows.

In Figure 2(a) and 2(b) we have plotted the luminosity function of the blue objects ($0.2 < (C-T_1) < 0.8$), which are mostly background galaxies (the dashed line). We have chosen this color range to avoid any contamination effect due to the faint blue globular clusters in deriving the luminosity function of the background galaxies. Figure 2(a) and (b) show that the luminosity function of the blue galaxies is negligible up to $T_1 \sim 23$ mag, but increases rapidly faintward from $T_1 \sim 23.2$ mag, showing a turnover at $T_1 \sim 24.9$ mag. which is close to the magnitude limit of our photometry. This turnover is undoubtedly due to the incompleteness of our photometry. It is of course impossible to distinguish individually globular clusters from unresolved background galaxies within our GCS color and magnitude limits. The color-magnitude diagram of faint field galaxies ($T_1 \gtrsim 23$ mag) in other fields shows that their color range is typically $-0.2 < (C - T_1) < 1.6$. Therefore it is concluded (a) that the contribution due to the field populations is, at most, minor, in the sample of the bright ($T_1 < 23$ mag) globular clusters, and in the sample of the RGCs up to the faint magnitude limit; but (b) that the field contamination starts to become significant faintward from $T_1 \sim 23.2$ mag in the BGCs.

Figure 2(a) and (b) display the luminosity function of the globular cluster candidates with $1.0 < (C - T_1) < 2.3$. The fainter part ($T_1 > 23.8$ mag) of this luminosity function is clearly affected by the contamination due to the background galaxies, as shown by the asymmetry around the peak. The contamination effect due to the background galaxies is reduced in the sample from which the bluest objects were removed. The luminosity functions of the objects with $1.3 < (C - T_1) < 2.3$ and the RGCs in Figure 2(a) and (b) illustrate this effect very well. Therefore, we have limited our GCLF analysis to objects brighter than $T_1 = 23.8$ with colors of $1.3 < (C - T_1) < 2.3$. Using these criteria, we feel that our data is sufficient to investigate the turnover in the GCLF, which lies at a bright enough magnitude that the various limitations are tractable.

Even though the luminosity functions of the various GC samples in Figure 2(b) show somewhat different shapes at the faint end, all three show clearly a peak at the same magnitude of $T_1 = 23.3 \pm 0.1$ mag. The bright part of the derived luminosity function of the globular clusters is well fit by a Gaussian function with a peak at $T_1 = 23.3$ mag and a width $\sigma = 1.3$, as shown in Figure 3. For this exercise, we fixed the width at a value typical of those found in giant elliptical GCSs (e.g. Whitmore *et al.* 1995) since we had the smallest leverage on this quantity, and derived a formal value of 23.31 ± 0.07 for the peak. Fixing the width at 1.4 increased the peak by only 0.03 mags.

Previous studies of the luminosity functions of the globular clusters in NGC 4472 were based on deep small field photometry (Cohen 1988, Harris *et al.* 1991). Cohen (1988) presented the g-band luminosity function of the globular clusters located in the radial range of $30'' < r < 300''$, and Harris *et al.* (1991) presented B-band luminosity functions of globular clusters in a $4'.1 \times 3'.4$ field centered on the nucleus of NGC 4472. We have compared these with ours in Figure 2(c). We have applied rough color relations appropriate for these globular clusters to convert g and B magnitudes into T_1 magnitudes for the purpose of comparison: $T_1 \sim B - 1.2$ and $T_1 \sim g - 0.55$ (Cohen 1988, Djorgovski & Meylan 1993). Figure 2(c) shows that the three sets of luminosity functions agree well in general, except for the fact that Cohen's shows some excess in the range of $23 < T_1 < 24$ mag compared with the other two. However, ours are based on a much larger number of globular clusters and deeper photometry than the others, but do suffer from the inability to perform image classification and background analysis. Also note that the Ajhar *et al.* (1994) data on NGC 4472 reveal a turnover at $R(\approx T_1) \sim 23.3$, in excellent agreement with our result.

3.3. The Peak Luminosity Difference between the BGCs and RGCs

We have investigated whether there is any systematic difference in the peak value of the luminosity functions of the BGCs and RGCs. The luminosity functions of the BGCs and RGCs are given in Table 2b and displayed in Figure 3. For the BGCs in Figure 3 we have counted only globular clusters with colors of $1.3 < (C - T_1) < 1.65$ instead of $1.0 < (C - T_1) < 1.65$ to reduce the field galaxy contamination at the faint end. The number of globular clusters in this sample is similar to that of the RGCs so that the two samples can be compared directly on a statistical basis. We have corrected these samples for the T_1 incompleteness but not for C incompleteness, and therefore it is likely that we are losing some of the reddest, faintest clusters. Figure 3 shows (a) that the shapes of the bright part of the luminosity function of the BGCs and RGCs are similar; (b) that the faint part of the luminosity function of the BGCs is more significantly affected by faint galaxies than that of the RGCs; and (c) that both the luminosity functions of the BGCs and RGCs show a peak at the same magnitude, $T_1 = 23.3$ mag. We are unable to quantify rigorously the similarity of these two peaks due to the various problems but estimate that they are the same to within ~ 0.15 mag.

Therefore it appears that there is little, if any, difference in the peak luminosities of the GCLFs of the BGCs and RGCs. This result is not consistent with the theoretical prediction by Ashman *et al.* (1995). According to the relations between peak luminosity vs. metallicity given by them, the peak luminosity of the RGCs should be 0.3 mag fainter in T_1 than that of the BGCs in the case of NGC 4472, which is not seen in Figure 3. This difference should be even larger in the more metallicity sensitive C filter. We have investigated this effect but are unable to make any useful comparison due to the data limitations.

In the case of M87, the cD galaxy in Virgo, the observational results published so far are somewhat confusing. Elson & Santiago (1996) suggested from the study of 254 globular clusters in a field $2'.5$ from the

center of M87 that the peak luminosity of the BGCs is 0.3 mag brighter than that of the RGCs. However, this conclusion is based on a small number of globular clusters. On the other hand, Whitmore *et al.* (1995) found only half this difference between the two populations from their study of 1032 globular clusters in a field $< 1'.7$ from the center of M87. The latter is consistent with our results on NGC 4472.

Finally, we note a curious feature seen clearly in Figure 1: in the brightest magnitude of the GCLF there are about twice as many BGCs as RGCs. This feature appears to be stronger than expected from the differences in population sizes but requires more study.

3.4. The Distance to NGC 4472

We have estimated the distance to NGC 4472 using the peak value of the luminosity function of the globular clusters obtained in the previous section, $T_1 = 23.3 \pm 0.1$ mag, in comparison with the luminosity function of the globular clusters in our Galaxy. Figure 2(d) displays the R-band luminosity function of the Galactic globular clusters which is derived from the compiled data of Djorgovski & Meylan (1993) and Harris (1996). We have plotted this figure in such a way that the position of the peaks in the GCLFs for NGC 4472 and our Galaxy are at the same location in the horizontal scale. We have adopted the metallicity-luminosity relation of the RR Lyraes of $M_V = 0.17[\mathrm{Fe/H}] + 0.82$, as discussed in Lee *et al.* (1993), in deriving the absolute magnitudes of the Galactic globular clusters. In Figure 2(d) we have plotted the luminosity functions for two samples: one for the halo globular clusters, the other for both halo and disk globular clusters. The luminosity functions of both samples of the Galactic globular clusters show clearly a peak at $M_R = -7.9 \pm 0.1$ mag (the difference between R and T_1 magnitudes is negligible (Geisler 1996)).

Comparing these peak values of the GCLFs we derive a distance estimate of $(m - M)_0 = 31.2 \pm 0.2$ for zero reddening (Burstein & Heiles 1982), which corresponds to a distance of 17.4 ± 1.6 Mpc. This distance estimate is consistent with the value based on the B-band GCLF (Harris *et al.* 1991), $(m - M)_0 = 31.3$, and the estimate based on the surface brightness fluctuation method, $(m - M)_0 = 31.18$ (Tonry 1990). However, our estimate is much larger than the value derived using the planetary nebula luminosity function, $(m - M)_0 = 30.7 \pm 0.19$ (Jacoby *et al.* 1990). Note that Ciardullo *et al.* (1993) presented later, in a comparative study of the planetary nebulae luminosity function and surface brightness fluctuation distance scales, updated values based on these two methods for NGC 4472: $(m-M)_0 = 30.84 \pm 0.11$ and 30.78 ± 0.07, respectively, which are significantly smaller than ours.

Our distance estimate for NGC 4472 is very similar to that for M87, the cD galaxy in the core of Virgo, $\approx 4^\circ$ away to the north of NGC 4472 (Lee & Geisler 1993a, Lee & Geisler 1993b, Whitmore *et al.* 1995). Lee & Geisler (1993b) estimated, from deep Washington CCD photometry, a peak GCLF value of $T_1 = 23.4 \pm 0.2$ mag (corresponding approximately to $V = 23.85$ mag). This estimate was confirmed later by more comprehensive data from Whitmore tal (1995) based on Hubble Space Telescope observations of over 1000 globular clusters in the central region of M87, who derived $V_{TO} = 23.72 \pm 0.06$ mag (Whitmore *et al.* 1995). Considering the foreground reddening of $E(B - V) = 0.02$ for M87 (Burstein & Heiles 1984) and adopting the same peak luminosity of the Galactic globular clusters as used for NGC 4472, we obtain an estimate for the distance modulus of M87 from the HST data, $(m - M)_0 = 31.2 \pm 0.1$. This value is slightly larger than the data from Whitmore *et al.* (1995), because they adopted an 0.1 mag fainter value for the peak luminosity of the Galactic globular clusters than that used in this study.

These results show that NGC 4472 and M87 are basically at the same distance from us, $d = 17.4 \pm 1.6$ Mpc, even though they are 4° apart in the sky. Adopting this value for the distance to Virgo yields

estimates for the Hubble constant, $H_0 = 68 \pm 6$ km s^{-1} for the Virgo velocity of 1179 ± 17 km s^{-1}(Jerjen & Tammann 1993), or $H_0 = 81 \pm 9$ km s^{-1} for the Virgo velocity of 1404 ± 80 km s^{-1}(Huchra 1988).

4. SPECIFIC FREQUENCY

The specific frequency, S_N, of the GCS of a galaxy is the total number of globular clusters ($N_{\rm tot}$) per unit galaxy luminosity ($M_V = -15$ mag), defined as $S_N = N_{\rm tot}10^{0.4(M_V^T+15)}$ (Harris & van den Bergh 1981). It represents the global efficiency of globular cluster formation over the history of the parent galaxy. We have estimated the specific frequency for NGC 4472 using the luminosity functions of the globular clusters given in the previous section as follows.

First, we calculate the total number of clusters which would have been observed in the CCD images, if the observations were deep enough to cover the faintest clusters. Assuming that the luminosity function is symmetric around the peak, we estimate the total number of globular clusters by doubling the number of observed clusters brighter than the peak luminosity, obtaining a value of 4116 clusters. Secondly, we estimate the correction due to lack of areal coverage for the central ($< 50''$) area and outer ($r > 420''$) area of NGC 4472, using the power-law and deVaucouleurs law for the radial profiles of the surface number density of the globular clusters obtained in the following section. We extrapolate the observed profiles out to $10'$.

We next estimate roughly the background level in our data considering the following: (a) The background level for NGC 4472 given by Harris (1986) is 4.3 objects per square arcmin for the magnitude limit of $V = 23.3$ mag (corresponding to $T_1 \sim 22.8$ mag); (b) In creating the globular cluster sample with colors $1.0 < (C - T_1) < 2.3$ we have already subtracted the non globular cluster candidates with colors $(C - T_1) < 1.0$ or > 2.3. Therefore we need to subtract only the field objects within the color range of the selected globular clusters from the globular cluster sample. Considering these two points, we derive roughly 2.4 objects per squarearcmin for the background level in our data. However, this value is much higher than the number density for the very outer area of the field ($500'' < r < 550''$) where some globular clusters are included. Therefore this value is considered as an upper limit to the background level.

Finally we derive the fully corrected total number of globular clusters in NGC 4472, obtaining 6700 ± 600 and 5500 ± 500 for the power-law and de Vaucouleurs law, respectively. The mean of these two values is 6100 ± 800, which is adopted as N_{tot} for the NGC 4472 GCS.

The total V magnitude of NGC 4472 is $V^T = 8.41$ mag (RC3), which corresponds to an absolute magnitude of $M_V^T = -22.8$ mag for the distance determined in the previous section, $d = 17.4 \pm 1.6$ Mpc. From the total number of globular clusters and the absolute magnitude of NGC 4472 we derive a value for the specific frequency, $S_N = 4.7 \pm 0.6$. A change in the distance modulus of +0.1 corresponds to a decrease in the specific frequency of -0.4.

Harris (1986, 1991) estimated the total number of globular clusters in NGC 4472 to be 7400 ± 2100, from the observed number of clusters with $V < 23.3$ mag, 2300 ± 400. He derived a specific frequency, $S_N = 5.0 \pm 1.4$ from these data for $(m - M)_0 = 31.3$. Our results are consistent with Harris' within the errors of the estimates, but ours have smaller errors than Harris' and are derived from a larger sample of clusters.

We have investigated the radial variation of the local specific frequency, as shown in Figure 4, which is also listed in Table 3. The surface photometry of the halo used in this diagram is described in Kim *et*

al. (1997). Figure 4 also displays the results given by McLaughlin *et al.* (1994) which were based on integrating the power law obtained from the luminosity function data of Harris (1986). McLaughlin *et al.* adopted a value for the distance modulus of $(m - M)_0 = 31.0$, which is 0.2 smaller than ours. Our results are consistent with McLaughlin *et al.*'s for an intermediate distance modulus, except in the outer regions, where our values fall substantially below his. McLaughlin *et al.*'s S_N values continue to increase even more than linearly with distance out to at least $20'$, reaching a value of ~ 32 at this radius. But note that this result is based on photographic GC and surface photometry data, and the latter only extend to $10'$. Given these limitations, we feel that the McLaughlin *et al.*'s specific frequency values beyond $\sim 8'$ are very uncertain, and in the outer parts represent a very large extrapolation. We find, instead, that S_N increases linearly with distance only out to $\sim 5.5'$, beyond which S_N levels off with a value of only about 8.5, some 4 times lower than the value derived by McLaughlin *et al.* for the outermost regions. Although our radial coverage does not extend beyond $7'$, it is difficult to believe that the local S_N would begin to increase again at some point. Note that McLaughlin *et al.*'s actual data for M87 shows a very similar behavior to that we find for NGC 4472 – a linear rise with radius out to about $7'$ with no further significant increase out to the limit of their data at about $9'$. The implications of these differences are quite important for some models of GC formation, as will be discussed in Section 6.

Our data allow us to investigate for the first time how the local specific frequency of the two GC populations vary with radius, as also shown in Figure 4. We see that both the RGCs and the BGCs increase their specific frequency linearly with radius from the central regions out to $\sim 5.5'$ and then level off with no further significant increase. Both of the populations have a very similar specific frequency in the inner regions but the BGC specific frequency increases more rapidly with radius than that of the RGCs, such that in the outer regions the specific frequency of the BGCs is $\sim$ twice that of the RGCs. Thus, if a galaxy with a GCS similar to that of NGC 4472 were subject to stripping, the stripped material would have a specific frequency ~ 8.5 and BGCs would outnumber RGCs by about a factor of 2.

5. SPATIAL STRUCTURE OF THE GLOBULAR CLUSTER SYSTEM

5.1. Overall Structure

We have investigated the spatial structure of the GCS in NGC 4472 using the final sample of the bright globular clusters with $T_1 < 23$. Figure 5 displays the spatial positions of these objects. Two important features are immediately seen in Figure 5: (1) The globular cluster candidates (5a) are centrally concentrated, while the non-globular cluster objects (5b - with the colors of $(C - T_1) < 1.0$ or $(C - T_1) > 2.3$) are uniformly distributed over the field; (2) The spatial distribution of the BGCs (5c) is clearly different from that of the RGCs (5d) in the sense that the latter is more spatially concentrated than the former. We also note a strong clumping of both the BGCs and RGCs in the inner NW and W directions, respectively. Similar clumpiness has been seen before in both the M87 and NGC 1399 GCSs (Pritchet 1996) but is presently not explained.

To investigate in detail the spatial structure of the globular cluster systems as seen in Figure 5, we have created globular cluster number density maps by counting globular clusters in a $24'' \times 24''$ reseau. Figure 6 illustrates the resulting cluster density contour maps. Note that the central region of 3×3 reseaus in Figure 6 is masked because of the saturated nucleus of NGC 4472. Figure 6(a) and (b) show that the spatial structure of the entire GCS is almost spherical in the outer area and somewhat elongated in the inner region, while the structure of the halo starlight of NGC 4472 is significantly elongated overall (with

ellipticity ~ 0.2 and position angle $150^\circ - 160^\circ$). Thus the overall structure of the entire GCS is different from that of the halo starlight.

Previously Harris & Petri (1978), from a photographic study of a region with $2' < r < 20'$, suggested that the GCS in NGC 4472 is almost spherically symmetric, while Cohen (1988) argued (from CCD data in a region with $0.5' < r < 5'$) that the GCS has the same ellipticity and position angle as the halo light. Our result indicates that the opposite conclusions given by these two studies are probably due to the mostly different radial ranges of NGC 4472 studied by them.

In addition, Figure 6(c) and 6(d) show striking evidence that the spatial structures of the BGCs and RGCs are systematically different: (1) The RGCs are more centrally concentrated than the BGCs; (note that the contour levels are the same in Figure 6(c) and (d)). (2) The spatial structure of the RGCs is significantly elongated roughly along the major axis of the halo of NGC 4472, while that of the BGCs is almost spherical. With a large sample of globular clusters in a wide field, we find for the first time that there are systematic differences in the spatial structure of the BGCs and RGCs in a giant elliptical galaxy. This is further strong evidence for the existence of two distinct populations of GCs in such a galaxy. Quantitative analysis of the spatial structure of the GCS follows.

5.2. Radial Structure

We have determined the structural parameters of the RGCs and BGCs, fitting ellipses to the number density maps of the globular clusters created as above. We have used the ellipse fitting routine ELLIPSE in IRAF/STSDAS for this purpose. Figure 7 displays the variation of the surface number density, color, ellipticity, and position angle with respect to the projected galactocentric radius for the two populations, and these results are listed in Table 4.

Surface number density: Figure 7(a) shows the radial profiles of the surface number density of the globular cluster systems we have derived. In Figure 8(a) we have compared our results for the entire GCS with Harris(1986)'s based on photographic counts of a wide field and Harris *et al.* (1991)'s based on CCD photometry of a small field close to the center of NGC 4472. In Figure 8(a) we have plotted the globular clusters brighter than $T_1 < 22.85$ mag, which is the limiting magnitude of the data in Harris (1986), and corrected our data for the background level derived above. These figures show that our results are roughly consistent with the other two in the overlapping radial range. We have fit the radial profiles of the entire GCS with $T_1 < 22.85$ mag using a power law and a deVaucouleurs law: $\log \sigma_{GC} = (1.60 \pm 0.04) - (1.23 \pm 0.06) \log r(\mathrm{arcmin})$ and $\log \sigma_{GC} = (3.16 \pm 0.12) - (1.62 \pm 0.08) r^{\frac{1}{4}}$ for the range of $70'' < r < 400''$. These coefficients are not significantly affected if we change from the $T < 22.85$ mag sample to the $T_1 < 23.0$ mag sample. In addition, Figure 7(a) shows that the surface number density of the RGCs decreases faster than that of the BGCs. We have fit the radial profiles of the BGCs and RGCs based on the original sample with $T_1 < 23.0$ mag. (i.e. uncorrected for background contamination), using the deVaucouleurs law and a power law, as shown in Figure 8(b): $\log \sigma_{GC} = (2.43 \pm 0.15) - (1.13 \pm 0.10) r^{\frac{1}{4}}$ (and $= (1.36 \pm 0.05) - (0.88 \pm 0.08) \log r$) for the BGCs and $\log \sigma_{GC} = (3.05 \pm 0.12) - (1.72 \pm 0.09) r^{\frac{1}{4}}$ (and $= (1.39 \pm 0.04) - (1.28 \pm 0.07) \log r$) for the RGCs. We have no information on the background levels for the BGCs and RGCs. In order to make a crude first-order correction, we assume the ratio of the background level for the BGCs and RGCs is one, and use the rough value for the background levels for $T_1 < 22.85$ mag sample. Figures 7(a) and 8(c) show the radial profiles after subtracting the background level from the number density for the BGCs and RGCs. Fitting similarly to these data, we

obtain $\log \sigma_{GC} = (2.75 \pm 0.17) - (1.42 \pm 0.12) r^{\frac{1}{4}}$ (and $= (1.40 \pm 0.06) - (1.12 \pm 0.09) \log r$) for the BGCs and $\log \sigma_{GC} = (3.66 \pm 0.19) - (2.28 \pm 0.14) r^{\frac{1}{4}}$ (and $= (1.47 \pm 0.06) - (1.73 \pm 0.11) \log r$) for the RGCs. Thus, the two populations have a spatial structure that differs at the $\sim 6\sigma$ level.

Color: Figure 7(b) shows that the median colors of the entire GCS show a strong radial gradient, while the RGCs and BGCs individually each show little, if any, radial gradient. The slopes (= d[Fe/H]/dlog r(arcmin)) determined in Paper I are -0.41 ± 0.03 for the entire GCS, -0.15 ± 0.03 for the BGCs, and -0.12 ± 0.06 for the RGCs. This indicates that the large radial gradient of the median colors of the entire GCS is simply due to the varying radial mixture of the two populations, rather than to dissipative processes, as discussed in detail in Paper I.

Ellipticity: Figure 7(c) shows that the mean ellipticity of the entire GCS is almost constant around the value of 0.16. The mean ellipticity of the RGCs increases from ≈ 0.06 continuously outward up to ≈ 0.3 at $r = 410''$. On the other hand, the ellipticity of the BGCs is almost constant around the value of 0.07, except for the range of $150'' < r < 240''$ where the ellipticities are as large as 0.27. The ellipticity for this range varies abruptly from nearby values. This variation is considered to be due to some local enhancement of the number density in the south east direction, as seen in Figure 6(c).

5.3. Azimuthal Structure

We have investigated the azimuthal distribution of the globular clusters. Figure 7(d) shows that the mean position angles of the entire GCS and the RGCs are similar with the value of about 150°. The position angles of the BGCs vary from $\sim 100°$ to $\sim 180°$. The significance of this large variation is small, considering the difficulty of accurate determination of the position angles for small ellipticities, as in this case. Figure 9 displays azimuthal variations of the globular cluster number density for the galactocentric radius of $70'' < r < 420''$. It shows that the entire GCS has an obvious peak at the position angle of $\approx 155°$, and that the RGCs have a peak at the same value, while the BGCs show an almost uniform distribution. The presence of only this one peak instead of two in Figure 9 is due to the asymmetric distribution of the globular clusters extended along the southeast direction.

5.4. Comparison of the Globular Cluster Populations with the Halo Light

We have compared the structural parameters of the globular cluster populations with those of the halo starlight of NGC 4472. The galaxy surface photometry is given in Kim *et al.* (1997). Note that our new results for the outer halo have changed significantly from those given in Paper I, due to a small change in the adopted C and T_1 background levels. Figure 7 reveals significant features as follows: (a) The radial profiles of the number density of the GCS are flatter than that of the halo, being spatially more extended than the halo. Note that the BGCs are significantly more extended than the halo, while the RGCs are marginally more extended than the halo. The T_1 surface brightness profiles are fit using the deVaucouleurs law and a power law, $\log \mu_{T_1} = (13.89 \pm 0.01) + (6.33 \pm 0.01) r^{\frac{1}{4}}$ and $\log \mu_{T_1} = (20.08 \pm 0.00) + (4.59 \pm 0.01) \log r$ (Kim *et al.* 1997). This slope of the halo is slightly steeper than the slope of the RGCs based on the background subtracted sample. However, the background level used for the RGCs is considered to be an overestimate, discussed in Section 4. Better estimation of the background level based on wider field imaging data is needed to obtain a more reliable estimate of the slope of the RGCs; (b) The median color of the RGCs is remarkably similar to that of the halo, while the median color of the BGCs is much bluer (by $\approx$0.5)

than that of the halo; (c) The mean ellipticity of the entire GCS is slightly smaller than that of the halo. The ellipticity of the RGCs becomes larger than that of the halo in the outer region, $r > 300''$, while the ellipticity of the BGCs is generally much smaller than that of the halo; (d) The mean position angle of the entire GCS is similar to that of the halo for $r > 200''$. In general, we see that the RGCs are more similar to the halo stars of NGC 4472 in terms of spatial structure and colors than are the BGCs.

6. SUMMARY AND DISCUSSION

Although it is risky to test galaxy formation models based on a single case, the fact is that our study of the NGC 4472 GCS represents the best data yet available which combines both deep widefield photometry, to ensure large samples and large radial coverage, as well as a wide color baseline that allows high metallicity precision. In particular, we have large numbers of both RGCs and BGCs with which to study their properties individually for the first time. Thus, although we strongly urge similar studies (and are carrying out such studies), we will examine the NGC 4472 GCS in some detail and compare our results to several GCS and galaxy formation models.

First, we summarize the salient observed characteristics of the NGC 4472 GCS as found in Paper I and this study:

1. The median metallicity of the entire GCS is [Fe/H]$= -0.9 \pm 0.2$ dex.
2. The GCS consists of two distinct populations: one metal-poor ([Fe/H] ~ -1.3 dex) and one metal-rich ([Fe/H] ~ -0.1 dex), with metallicity spreads in each population consistent with that of the halo GCs in our Galaxy (σ ([Fe/H])~ 0.35 dex).
3. The number ratio RGC/BGC = 0.6.
4. The luminosity function of the globular clusters shows a peak at $T_1 = 23.3 \pm 0.1$ mag.
5. The total number of globular clusters in NGC 4472 within $r \sim 10'$ is estimated to be 6100 ± 800, and the global specific frequency is $S_N = 4.7 \pm 0.6$. The local specific frequency increases linearly with radius from ~ 1.5 at $r = 1'$ to ~ 8.5 at $r \sim 5.5'$ but does not increase further beyond this distance, to at least $7'$. Both the RGCs and the BGCs show similar radial trends, with the local specific frequency of the BGCs increasing more rapidly with radius such that in the outer regions there are about twice as many BGCs as RGCs.
6. The RGCs are more centrally concentrated than the BGCs. The BGCs are significantly more extended than the halo, while the RGCs are marginally more extended than the halo
7. The metallicity gradient of the entire GCS is Δ[Fe/H]$/\Delta \log r = -0.41 \pm 0.03$, but most of this gradient appears to be due to the varying radial concentration of the two populations, and not to dissipative processes, since neither the RGCs or the BGCs show significant gradients.
8. The color of the RGCs is remarkably similar to that of the halo starlight, while the color of the BGCs is much bluer than that of the halo star light, indicating a metallicity difference of [Fe/H]~ 1.2 dex.
9. The spatial structure of the entire GCS is almost spherical in the outer region and somewhat elongated in the inner region. The BGCs are distributed almost spherically, while the RGCs are elongated along the major axis of the halo star light.

These results can be used as constraints on models for the origin of globular clusters. There have been several models suggested, a brief summary of which is given in Ashman & Zepf (1997) and Forbes *et al.* (1997 - hereafter FBG97). Here we consider only two models: the gaseous merger model (Ashman & Zepf 1992 - hereafter AZ92, Zepf & Ashman 1993, see also Hernquist & Bolte 1993) and the episodic *in situ* formation plus tidal stripping model (FBG97).

In the gaseous merger model, an elliptical galaxy is formed by the merging of two or more gas-rich spiral galaxies. The spiral galaxies have enriched gas in the disk and metal-poor globular clusters in the halo. New globular clusters are formed from the enriched gas during the merging/interacting process. The resulting elliptical galaxy then has two GC populations: the younger, more metal-rich, and spatially more concentrated clusters formed as a result of the merger, and the original, metal-poor, more spatially extended GCs formed in the progenitor spirals. It is generally true that typical cluster ellipticals have a $\gtrsim$ factor of 2 higher specific frequency than spirals. (However, we note the need for more complete studies of even nearby galaxies, using large area detectors in order to study the entire GCS to fainter magnitude levels than in previous studies, and thus improve existing S_N values.) In order to account for the $\gtrsim$ factor of 2 higher specific frequency of ellipticals compared to spirals, which is a key idea of the merger model as proposed by AZ92, at least as many new RGCs are needed to be made in the merger as were originally present in the combined total of BGCs in the progenitor spirals.

This merger model has been very successful in explaining several observed qualitative characteristics of the globular clusters in giant elliptical galaxies and interacting galaxies: for example, the presence of young massive clusters in interacting galaxies (e.g. Whitmore & Schweizer 1995), the bi(or multi)-modal metallicity distributions in a number of GCSs (Paper I, FBG97), and the lack of metallicity gradients in either of the two populations but the presence of a gradient in the overall GCS (e.g. Paper I). However, some of the quantitative predictions of the AZ92 model have not been born out by recent observations. This was recently pointed out by FBG97. In particular, the number of RGCs found in most multimodal ellipticals known is insufficient to explain the specific frequency differences between typical spirals and ellipticals. In addition, the global specific frequency is roughly anticorrelated with the number ratio N_{RGC}/N_{BGC}, opposite to the prediction of AZ92.

To explain such findings, FBG97 proposed another model, the episodic *in situ* formation plus tidal stripping model. In this model metal-poor globular clusters are formed first at an early stage in the initial collapse of the protogalactic cloud with only minor star formation. After some time (≈ 4 Gyrs) of quiescence, metal-rich globular clusters are formed out of more enriched gas, roughly contemporaneously with most of the galaxy stars, during the major collapse of the protogalactic cloud, which then forms an elliptical galaxy with two GC populations. Most of the globular clusters are formed in the first formation episode and should not be structurally related to the halo light, while the newly formed globular clusters are closely coupled to the galaxy and share a common chemical enrichment history and structural characteristics.

We will discuss each of our above salient points of relevance to these two theories in turn:

Point 2. The existence of multimodal GC populations in giant ellipticals is now known to be widespread (Paper I, FBG97) and perhaps universal. The merger model **predicted** this and is one of its major successes, while FBG97 use this as an initial theorem from which they derive their model. As pointed out by FBG97, the existence of multimodality rules out simple monolithic collapse models since these would form only a single population of GCs. However, the similar metallicity spreads in each population and the constancy of the metallicity difference between them in different galaxies is something that requires both additional observational confirmation (this indeed applies to all of our points) and theoretical explanation.

For example, a giant elliptical having suffered many mergers would be expected to possess very broad metallicity ranges as opposed to the distinct, rather narrow peaks that are seen.

Point 3. As in our data on NGC 4472, of the ~ 13 well studied giant ellipticals to date (FBG97, Geisler & Lee 1998, Lee & Geisler 1998), only two have $N_{RGC}/N_{BGC} \gtrsim 1$, as required by the merger model. Most cases show a ratio of only ~ 0.5, a factor of 2 or more lower than needed to explain the specific frequency differences. This is an obvious blow to the original AZ92 model.

Point 5. The *in situ* scenario predicts that higher specific frequency values should be associated with the BGCs, since they formed at a time when cluster formation dominated star formation, and this agrees with our finding of higher specific frequency for the BGCs in the outer regions of the NGC 4472 GCS. However, FBG97 also invoke stripping of the outer regions of nearby galaxies to account for the unusually high specific frequency values associated with some cD galaxies, such as M87, and refer to McLaughlin *et al.*'s (1994) work to state that the outer regions of some ellipticals, and NGC 4472 in particular, have a very high specific frequency, as much as in the outer regions of M87. However, we have seen that the outer regions of NGC 4472 probably have a specific frequency about 4 times lower than the value derived by McLaughlin *et al.*, which makes it much more difficult to build up large specific frequency galaxies from stripping of the outer regions of a GCS like that of NGC 4472.

Point 6. Both models predict that the RGCs will be more centrally concentrated than the BGCs. The *in situ* model further predicts that the RGCs should have the same spatial distribution as the galaxy halo. The RGCs are marginally more extended than the halo light.

Point 7. Both models predict a metallicity gradient in the overall GCS due to the varying concentration of the two populations. The *in situ* model would further predict that the RGCs should also show a gradient due to dissipation, which is not seen in NGC 4472.

Point 8. Both models successfully predict the close agreement of the metallicity of the RGCs and the galaxy light, and the offset of these from the BGCs.

Point 9. Both models would predict a roughly spherical distribution of the BGCs. FBG97 also predict that the RGCs will closely match the ellipticity of the underlying galaxy, as seen in NGC 4472. The merger model would also suggest that these distributions should be similar, but results may depend on details of the merger.

FBG97 also predicted that the RGCs should show some rotation, depending on the amount of dissipation, while the BGCs should have no rotation and a large velocity dispersion. Kinematic studies of a large number of the BGCs and RGCs in NGC 4472 are required to test these predictions (Mould *et al.* (1990) measured the velocities of 26 globular clusters in NGC 4472, but the number of clusters is too small to study the differences between the metal-poor and metal-rich systems.) Such studies are indeed now becoming available: e.g. Sharples *et al.* (1997) have obtained spectra of 57 GCs in NGC 4472, with roughly equal numbers of BGCs and RGCs. They find no sign of rotation in either population, and a strong hint that the BGCs have a higher velocity dispersion than the RGCs.

Thus, we see that both models have some successes as well as failures when compared to observations. FBG97 point out several other problems with the merger model. However, as they admit, their scenario lacks an explanation for why star and cluster formation was shut down for several Gyrs and why it was then reinitiated. In our view, it is now becoming increasingly clear that mergers are involved in the formation of many giant ellipticals and that a natural explanation of the onset of the second generation of star and cluster formation is provided by mergers. However, it is also now quite clear that this second generation of

clusters was in general insufficient to make up the difference in specific frequency between typical spirals and ellipticals. Thus, the AZ92 merger model may well explain the second epoch trigger mechanism, but, ironically, we may still be left with the original problem they tried to solve – how to account for the specific frequency difference. The question of the origin of the high specific frequency GCSs remains outstanding.

D.G. would like to acknowledge the Department of Astronomy, Seoul National University, and E. Geisler for their kind hospitality, and understanding and patience, respectively, during his stay there. This research is supported by NON DIRECTED RESEARCH FUND, Korea Research Foundation, 1996 (to M.G.L.). This research is supported in part by NASA through grant No. GO-06699.01-95A (to D.G.) from the Space Telescope Science Institute, which is operated by the Association of Universities for Research in Astronomy, Inc., under NASA contract NAS5-26555.

REFERENCES

Ajhar, E. A., Blakeslee, J. P., & Tonry, J. L. 1994, AJ, 108, 2087

Ashman, K.M., & Zepf, S. E. 1992, ApJ, 384, 50 (AZ92)

Ashman, K.M., & Zepf, S.E. 1997, Globular Cluster Systems, Cambridge University Press, in press

Ashman, K.M., Conti, A., & Zepf, S. E. 1995, AJ, 110, 1164

Burstein, D., & Heiles, C. 1982, AJ, 87, 1165

Burstein, D., & Heiles, C. 1984, ApJS, 54, 33

Canterna, R. 1976, AJ, 81, 228

Ciardullo, R., Jacoby, G. H., & Tonry, J. L. 1993, ApJ, 419, 479

Cohen, J. G. 1988, AJ, 95, 682

Couture, J., Harris, W. E., & Allwright, J. W. B. 1991, AJ, 372, 97

de Vaucouleurs, G., de Vaucouleurs, A., Corwin, H. G., Jr., Buta, R. J., Paturel, G., & Fouqué, P. 1991, Third Reference Catalogue of Bright Galaxies (Springer-Verlag, New York) (RC3)

Djorgovki, G. ,& Meylan, G. 1993, in ASP Conf. Ser. 50, Structure and Dynamics of Globular Clusters, eds. G. Djorgovski & G. Meylan, (ASP, San Francisco), 337, 373

Elson, R. A. W., & Santiago, B. X. 1996, MNRAS, 280, 971

Forbes, D. A., Brodie, J. P., & Grillmair, C. J. 1997, AJ, 113, 1652 (FBG97)

Geisler, D., 1996, AJ, 111, 480

Geisler, D., & Lee, M. G. 1998, in preparation

Geisler, D., Lee, M. G., & Kim, E. 1996, AJ, 111, 1529 (Paper I)

Harris, W. E. 1986, AJ, 91, 822

Harris, W. E. 1991, ARA&A, 29, 543

Harris, W. E. 1996, AJ, 112, 1487

Harris, W. E., & Petrie, P. L. 1978, ApJ, 223, 88

Harris, W. E., & van den Bergh, S. 1981, AJ, 86, 1627

Harris, W. E., Allwright, W. B., Pritchet, C. J., & van den Bergh, S. 1991, ApJS, 76, 115

Hernquist, L., & Bolte, M. 1993, in ASP Conf. Ser. 48, The Globular Cluster-Galaxy Connection, ed. G. Smith & J. Brodie, (ASP, San Francisco), 472

Huchra, J. 1988, in ASP Conf. Ser. 4, Estragalactic Distance Scale, ed. S. van den Bergh and C. J. Pritchet (ASP, San Francisco), 257

Jacoby, G. H., Ciardullo, R., & Ford, H. C. 1990, ApJ, 356, 332

Jacoby, G. H., Branch, D., Ciadullo, R., Davis, R. L., Harris, W. E., Pierce, M. J., Pritchet, C. J., Tonry, J. L., & Welch, D. L. 1992, PASP, 104, 599

Jerjen, H., & Tammann, G. A. 1993, A&A, 273, 354

Kim, E., Lee, M. G., & Geisler, D. 1996, IAU Symp. No. 174, Dynanamical Evolution of Star Clusters, eds. P. Hut and J. Makino, (Kluwer, Dordrecht), 391

Kim, E., Lee, M. G., & Geisler, D. 1997, in preparation.

Lee, M. G., & Geisler, D. 1993a, AJ, 106, 423

Lee, M. G., & Geisler, D. 1993b, in ASP Conf. Ser. 48, The Globular Cluster-Galaxy Connection, ed. G. Smith & J. Brodie, (ASP, San Francisco), 576

Lee, M. G., & Geisler, D. 1998, in preparation

Lee, M. G., Freedman, W. L. & Madore, B. F. 1993, ApJ, 417, 553

Lee, M. G., Kim, E., & Geisler, D. 1996, in IAU Symp. No. 174, Dynanamical Evolution of Star Clusters, eds. P. Hut and J. Makino, (Kluwer, Dordrecht), 393

McLaughlin, D. E., Harris, W. E., & Hanes, D. A. 1994, ApJ, 422, 486

Mould, J. R., Oke, J. B., de Zeeuw, P. T., & Nemec, J. M. 1990, AJ, 99, 1823

Pritchet, C. J. 1996, private communication

Sharples, R., *et al.* 1997, in preparation

Strom, S. E., Forte, J. C., Harris, W. E., Strom, K. M., Wells, D. C., & Smith, M. G 1981, ApJ, 245, 416

Tonry, J. 1990, AJ, 100, 1416

Whitmore, B.C., & Schweizer, F. 1995, AJ, 109, 960

Whitmore, B. C., Sparks, W. B., Lucas, R. A., Macchetto, F. D., & Biretta, J. A. 1995, ApJ, 454, L73

Zepf, S. E., & Ashman, K. M. 1993, MNRAS, 264, 611

Table 1. Completeness of photometry.

C	$f(C)$	ΔC	σ_C	T_1	$f(T_1)$	ΔT_1	σ_{T_1}
20.28	1.00	0.002	0.005	18.17	1.00	−0.002	0.000
20.78	1.00	0.000	0.004	18.67	1.00	−0.001	0.003
21.28	1.00	0.001	0.005	19.17	1.00	0.000	0.004
21.78	1.00	0.002	0.009	19.67	1.00	0.001	0.006
22.28	1.00	0.003	0.010	20.17	1.00	0.001	0.007
22.78	1.00	0.002	0.017	20.67	1.00	0.000	0.008
23.28	1.00	0.004	0.026	21.17	1.00	0.002	0.014
23.78	0.99	0.000	0.040	21.67	1.00	0.005	0.020
24.28	0.98	0.003	0.061	22.17	1.00	0.005	0.035
24.78	0.96	0.002	0.093	22.67	0.98	0.003	0.057
25.28	0.84	−0.002	0.142	23.17	0.96	0.006	0.082
25.78	0.61	−0.047	0.207	23.67	0.95	0.007	0.128
26.28	0.33	−0.178	0.297	24.17	0.78	−0.002	0.180
26.78	0.13	−0.390	0.316	24.67	0.47	−0.100	0.277
				25.17	0.21	−0.334	0.311
				25.67	0.09	−0.638	0.292

Table 2a. Luminosity function of all measured globular clusters in NGC 4472.

T_1	$N(T_1)$	T_1	$N(T_1)$	T_1	$N(T_1)$	T_1	$N(T_1)$
19.5	6	20.7	34	21.9	102	23.1	195
19.7	10	20.9	48	22.1	99	23.3	214
19.9	11	21.1	62	22.3	134	23.5	193
20.1	11	21.3	64	22.5	146	23.7	165
20.3	21	21.5	76	22.7	168		
20.5	20	21.7	94	22.9	163		

Table 2b. Luminosity function of blue and red globular clusters in NGC 4472.

	$N(T_1)$			$N(T_1)$	
T_1	BGC	RGC	T_1	BGC	RGC
19.65	6.0	3.3	21.75	42.7	54.7
19.95	8.0	2.7	22.05	50.0	50.0
20.25	10.7	7.3	22.35	57.1	77.9
20.55	11.3	12.7	22.65	73.4	91.8
20.85	25.3	20.0	22.95	81.2	89.5
21.15	39.3	25.3	23.25	105.0	106.4
21.45	38.0	32.7	23.55	96.6	79.8

Table 3. Radial variaton of the local specific frequency of the globular clusters in NGC 4472.

R [arcsec]	S_N	R [arcsec]	S_N
72	1.59 ± 0.09	283	5.78 ± 0.34
107	2.56 ± 0.14	313	7.40 ± 0.44
137	3.77 ± 0.21	339	8.60 ± 0.52
167	4.01 ± 0.23	368	8.87 ± 0.55
196	5.15 ± 0.29	398	8.71 ± 0.57
224	5.20 ± 0.30	433	8.66 ± 0.57
252	5.88 ± 0.34		

Table 4. Radial surface density of the globular cluster system in NGC 4472.

ALL		BGC		RGC	
R[arcsec]	σ_{GC}	R[arcsec]	σ_{GC}	R[arcsec]	σ_{GC}
54	31.4 ± 3.1	61	14.6 ± 1.8	50	15.1 ± 2.5
97	24.3 ± 2.4	111	12.0 ± 1.5	84	15.3 ± 2.6
131	21.2 ± 2.1	146	11.8 ± 1.5	111	10.2 ± 1.7
164	15.3 ± 1.5	181	7.6 ± 1.0	138	9.7 ± 1.6
196	14.4 ± 1.4	215	8.5 ± 1.1	165	6.7 ± 1.1
227	12.3 ± 1.2	245	6.8 ± 0.9	196	5.3 ± 0.9
257	11.4 ± 1.1	277	6.2 ± 0.8	228	4.4 ± 0.7
289	8.4 ± 0.8	308	5.6 ± 0.7	260	3.9 ± 0.7
324	7.7 ± 0.8	338	5.2 ± 0.7	296	2.8 ± 0.5
357	7.7 ± 0.8	369	4.7 ± 0.6	334	2.6 ± 0.4
391	6.1 ± 0.6	404	3.4 ± 0.4	371	2.3 ± 0.4
430	4.6 ± 0.5	440	1.9 ± 0.2	414	1.7 ± 0.3

The surface densities are given in units of number per arcmin^2 for the sample with $T_1 < 23.0$ mag.

Table 5. Structural parameters of the globular cluster system in NGC 4472.

R [arcsec]	Ellipticity			Position Angle		
	ALL	BGC	RGC	ALL	BGC	RGC
72	0.03 ± 0.04	0.05 ± 0.05	0.07 ± 0.04	135±36	184±29	113±15
120	0.12 ± 0.06	0.05 ± 0.08	0.06 ± 0.07	134±14	106±47	143±34
168	0.11 ± 0.07	0.26 ± 0.08	0.06 ± 0.06	144±18	124±10	151±32
216	0.17 ± 0.07	0.28 ± 0.08	0.12 ± 0.09	153±14	132±10	156±23
264	0.20 ± 0.08	0.08 ± 0.09	0.21 ± 0.09	149±12	137±35	143±14
312	0.14 ± 0.07	0.03 ± 0.10	0.24 ± 0.09	132±15	20±83	135±12
360	0.19 ± 0.06	0.13 ± 0.07	0.28 ± 0.09	149±10	165±16	137±11
408	0.20 ± 0.04	0.08 ± 0.09	0.31 ± 0.07	151±6	184±34	141±8
456	0.13 ± 0.08	0.05 ± 0.11	0.31 ± 0.06	164±21	205±62	144±6

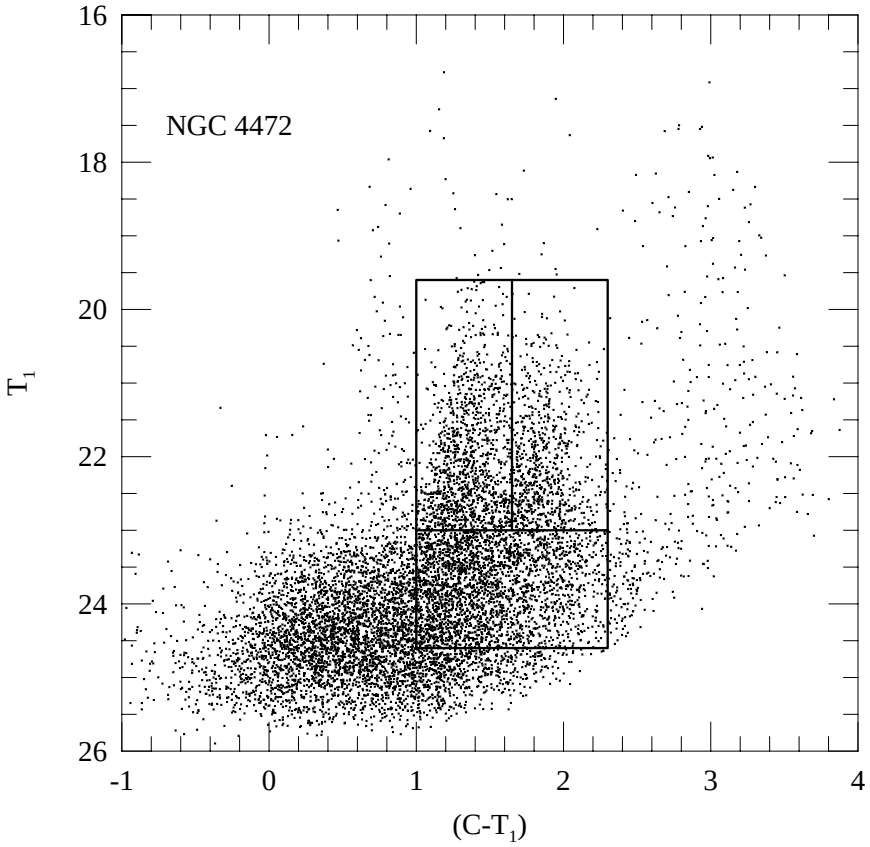

Fig. 1.— T_1 vs. $(C - T_1)$ diagram of all objects from Paper I. The boundaries for the blue globular clusters (BGCs) and red globular clusters (RGCs), as defined in Paper I, are marked by the boxes. The middle horizontal line marks the lower limit of our bright GC sample used to study the GCS spatial structure, while the lower line indicates the completeness limit of our photometry.

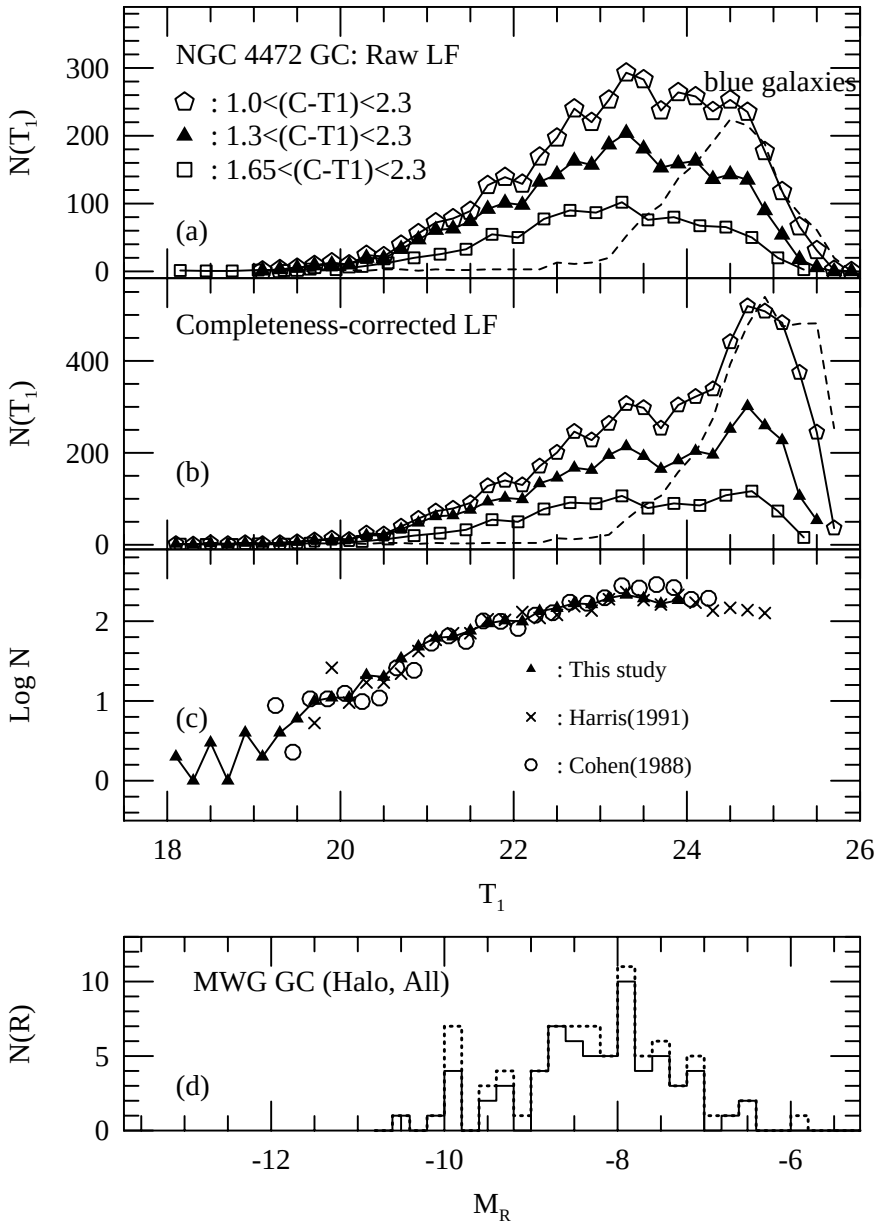

Fig. 2.— (a) T_1 luminosity functions of the globular clusters in NGC 4472 before completeness correction (the pentagons: $1.0 < (C-T_1) < 2.3$; the triangles: $1.3 < (C-T_1) < 2.3$;and the squares: $1.65 < (C-T_1) < 2.3$). The dashed line represents the luminosity function of the blue objects with $0.2 < (C-T_1) < 0.8$ which are mostly background galaxies. (b) Completeness-corrected luminosity functions. Note that our results have not been corrected for background contamination, and are unreliable for $T_1 > 23.8$; (c) Comparison of our results (the triangles) with previous studies. The circles and crosses represent the g-band data given by Cohen (1988) and the B-band data given by Harris *et al.* (1991), respectively. These two sets of data were arbitrarily moved along the vertical direction to match with ours around $T_1 = 23$ mag, and along the horizontal direction according to the magnitude relations as described in the text. We have limited our data to $T_1 < 23.8$. (d) R luminosity function of the Galactic globular clusters (the solid line: halo globular clusters, and the dotted line: both halo and disk globular clusters).

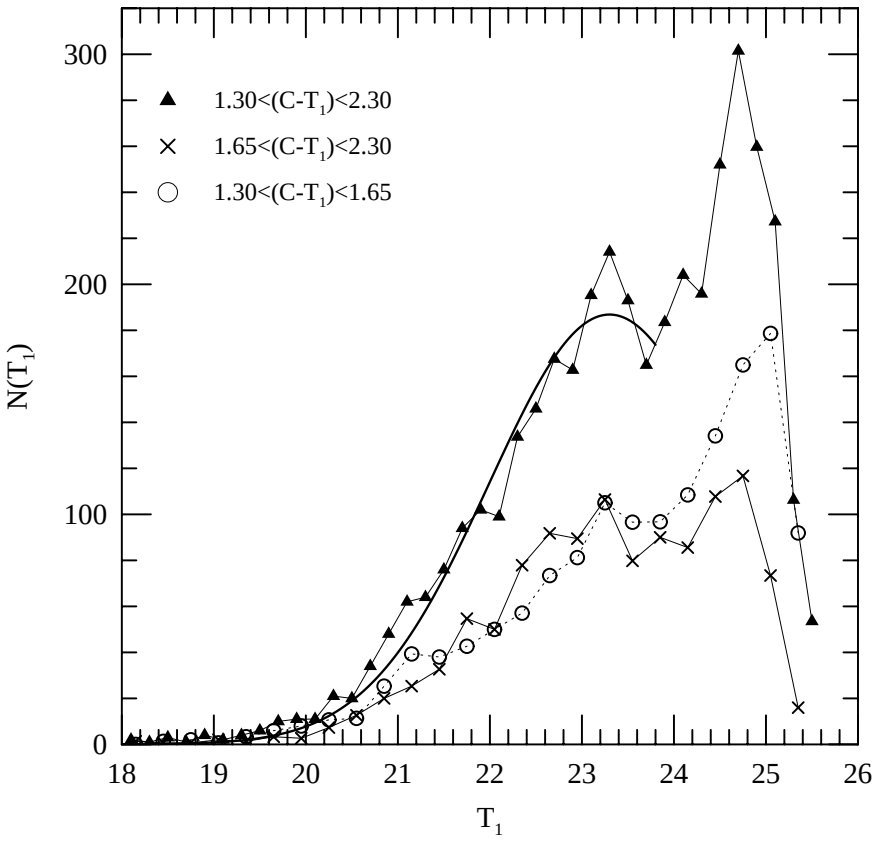

Fig. 3.— Comparison of the luminosity functions for the GCs with $1.3 < (C - T_1) < 2.3$ (triangles), the BGCs with $1.3 < (C - T_1) < 1.65$ (the circles) and the RGCs (the crosses). The solid line represents a Gaussian fit to the luminosity function of the globular clusters with $1.3 < (C - T_1) < 2.3$, and has a peak at $T_1 = 23.31$ mag and $\sigma = 1.3$.

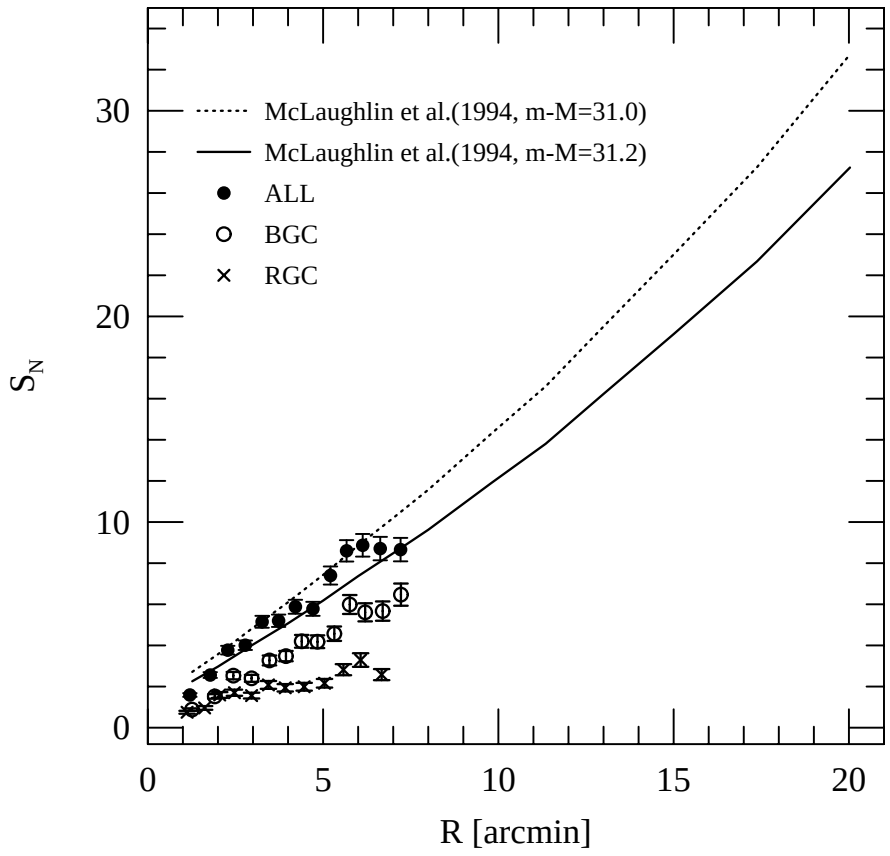

Fig. 4.— Radial variation of the local specific frequency. The dashed line represents the results given by McLaughlin *et al.* (1994), and the solid line represents the same results adjusted for the distance modulus of NGC 4472 obtained in this study. Open circles are for the BGCs, crosses for RGCs and filled circles for the combined sample. Error bars include both Poisson errors in the GC counts and errors in the surface photometry.

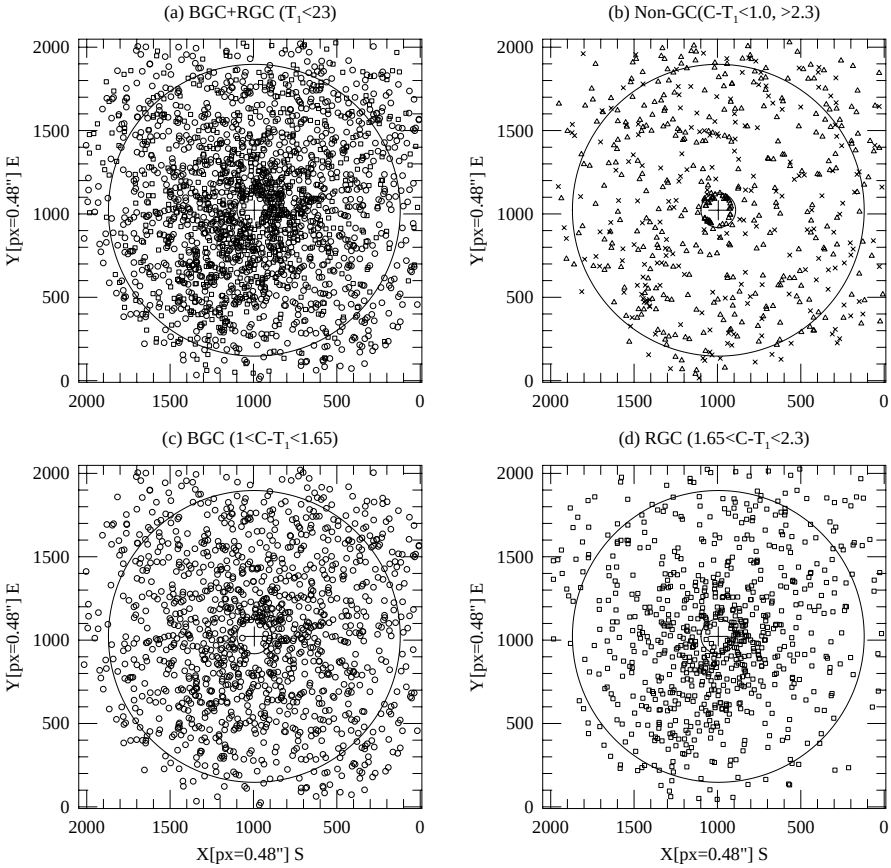

Fig. 5.— Positions of the measured objects with $T_1 < 23$ mag in the field. The cross represents the center of NGC 4472, and the circles with radii of 63 pixels (=50″) and 875 pixels (=420″) represent the boundary of the region used for the final sample in this study. (a) All globular clusters. (b) Very blue (the crosses) or very red (the triangles) objects which are foreground stars or background galaxies. (c) The BGCs. (d) The RGCs.

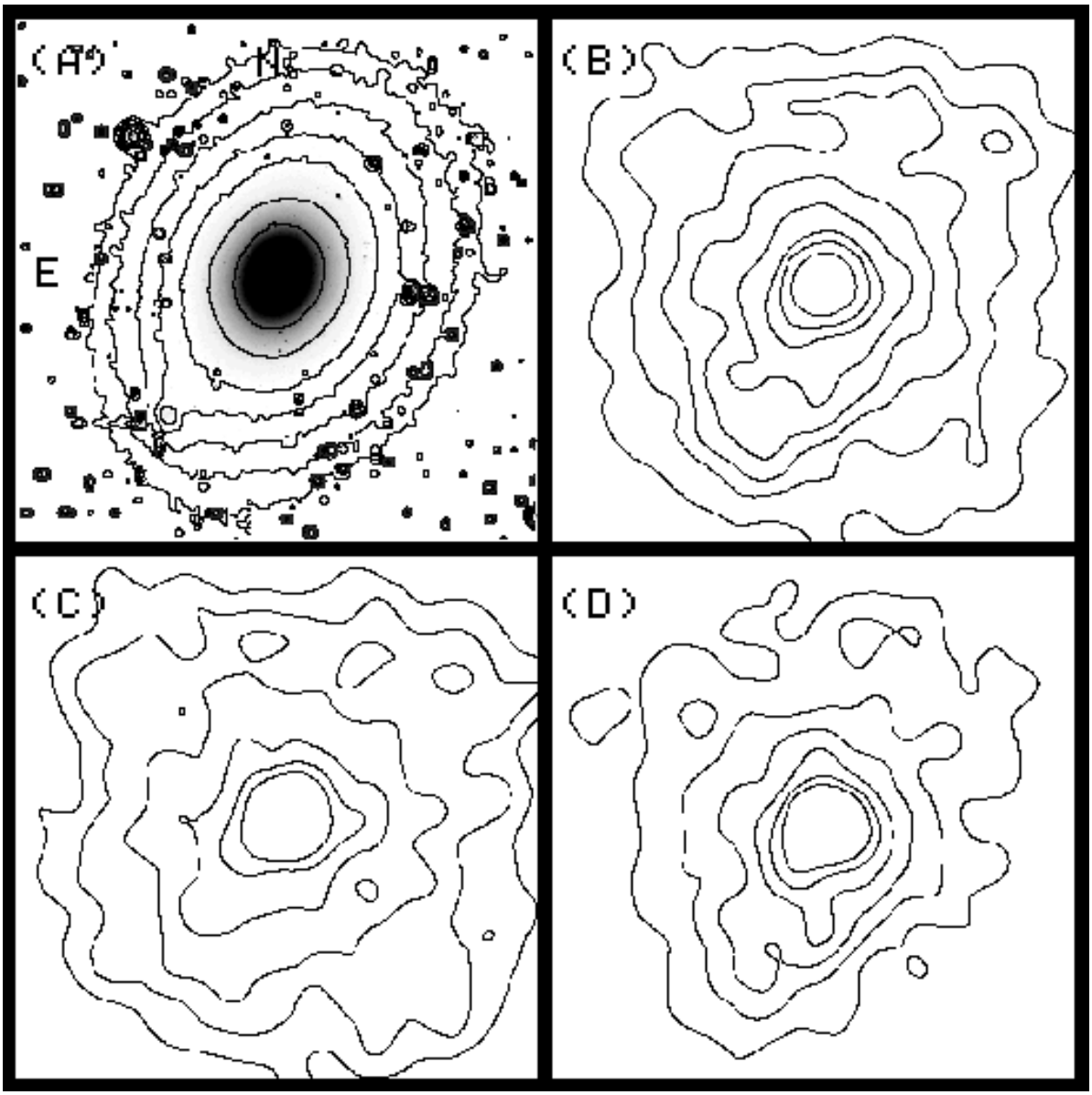

Fig. 6.— A greyscale map of a short exposure T_1 CCD image of NGC 4472 (a), and surface number density maps for the globular clusters with $T_1 < 23$ mag ((b) the entire GCs, (c) the BGCs and (d) the RGCs). The contour levels are 3.1, 6.3, 8.8, 12.5, 17.5, 25.0, 31.3, and 43.8 objects/arcmin^2 for (b) and 1.9, 3.8, 6.3, 9.4, 12.5 and 15.6 objects/arcmin^2 for (c) and (d).

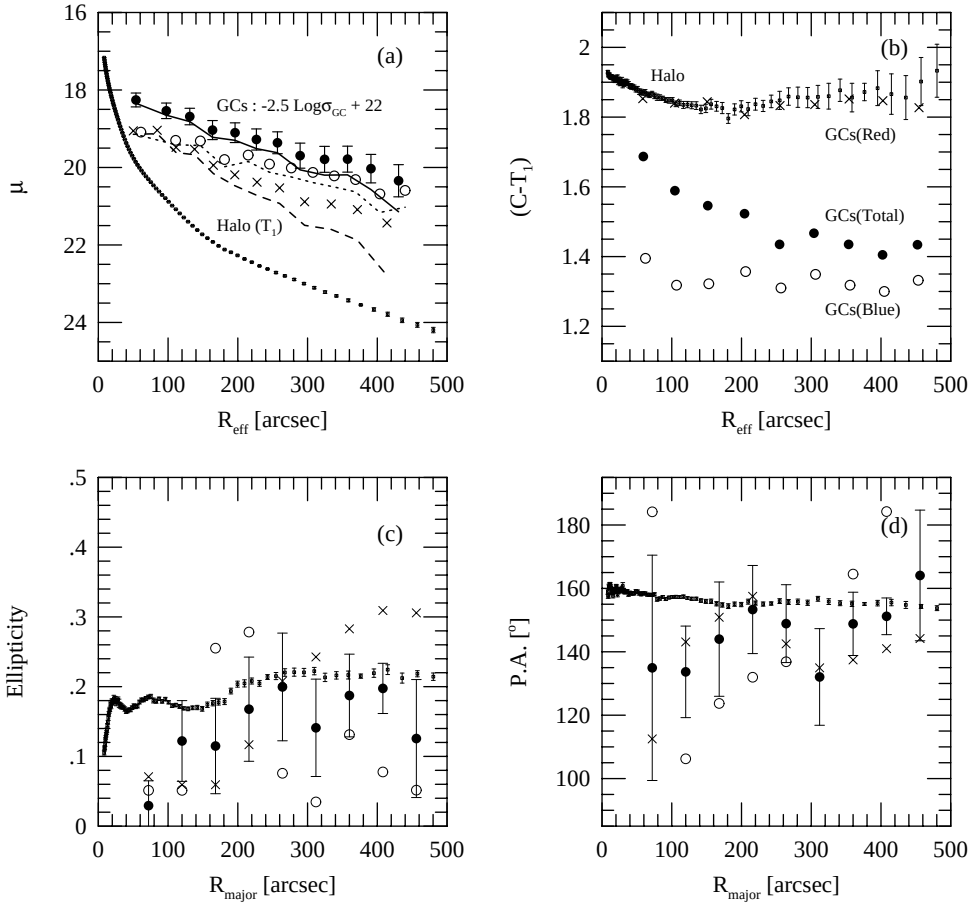

Fig. 7.— Radial variations of the surface number density, color, ellipticity, and position angle of the globular clusters in NGC 4472. The filled circles, open circles and crosses represent, respectively, the entire GCS, the BGCs and the RGCs. Also shown as small squares with error bars are the surface brightness and other parameters for the halo light of NGC 4472. In (a), both the raw data points as well as the background-subtracted data (solid, dotted and dashed lines, respectively) are shown.

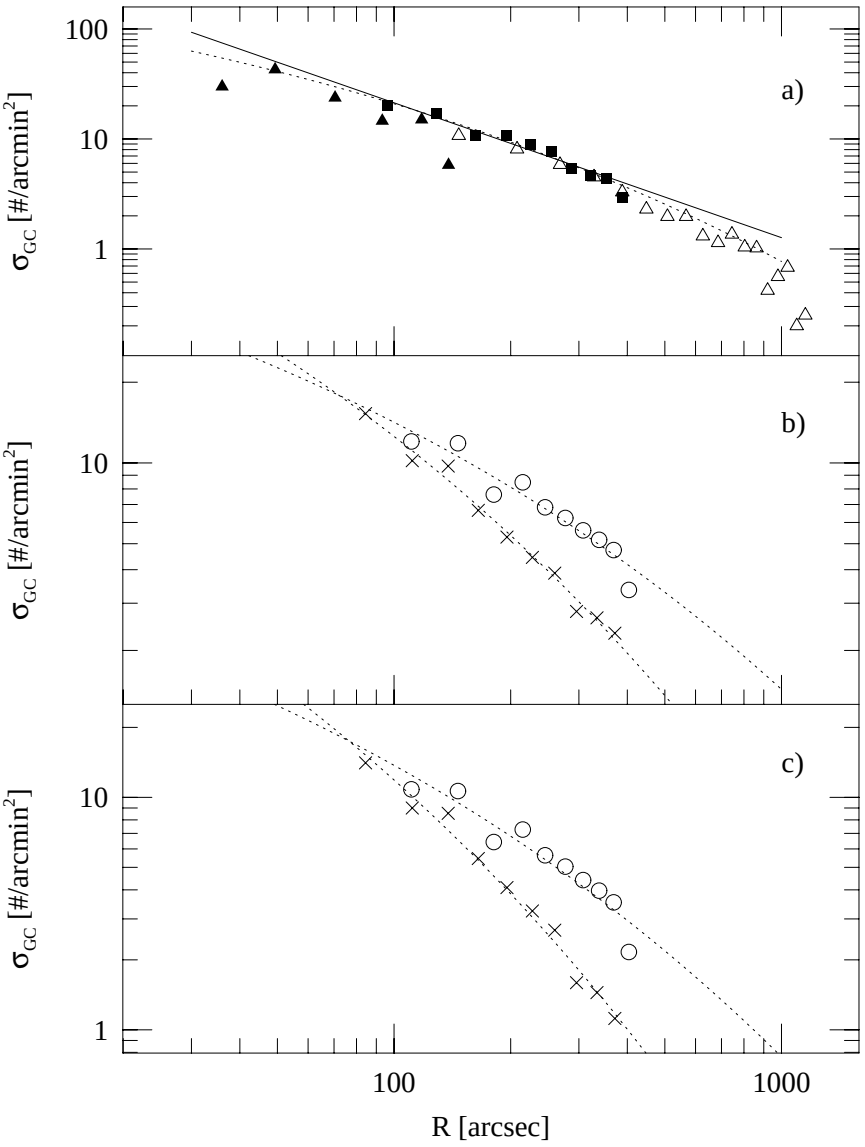

Fig. 8.— (a) Comparison of this study and previous studies of the radial variation of the surface number density of the globular clusters in NGC 4472. (the filled squares: the entire GCS with $T_1 < 22.85$ mag in this study after background subtraction; the open triangles: Harris (1986); the filled triangles: Harris *et al.* (1991)). Note that we have shown here only globular clusters brighter than $T_1 = 22.85$ mag which is the limiting magnitude of the Harris(1986)'s data, while the limiting magnitude of the Harris *et al.* (1991)'s data is $T_1 \sim 23.24$ mag. The solid line and dotted line represent the fits with a power law and a deVaucouleurs law, respectively. (b) Comparison of the radial profiles of the metal-poor GCS (the open circles) and metal-rich GCS (the crosses) with $T_1 < 23$ mag, with no background subtraction. The dotted lines represent the fits with a deVaucouleurs law. (c) Comparison of the radial profiles of the metal-poor GCS (the open circles) and metal-rich GCS (the crosses) with $T_1 < 23$ mag from which the background level was roughly subtracted. The dotted lines represent the fits with a deVaucouleurs law.

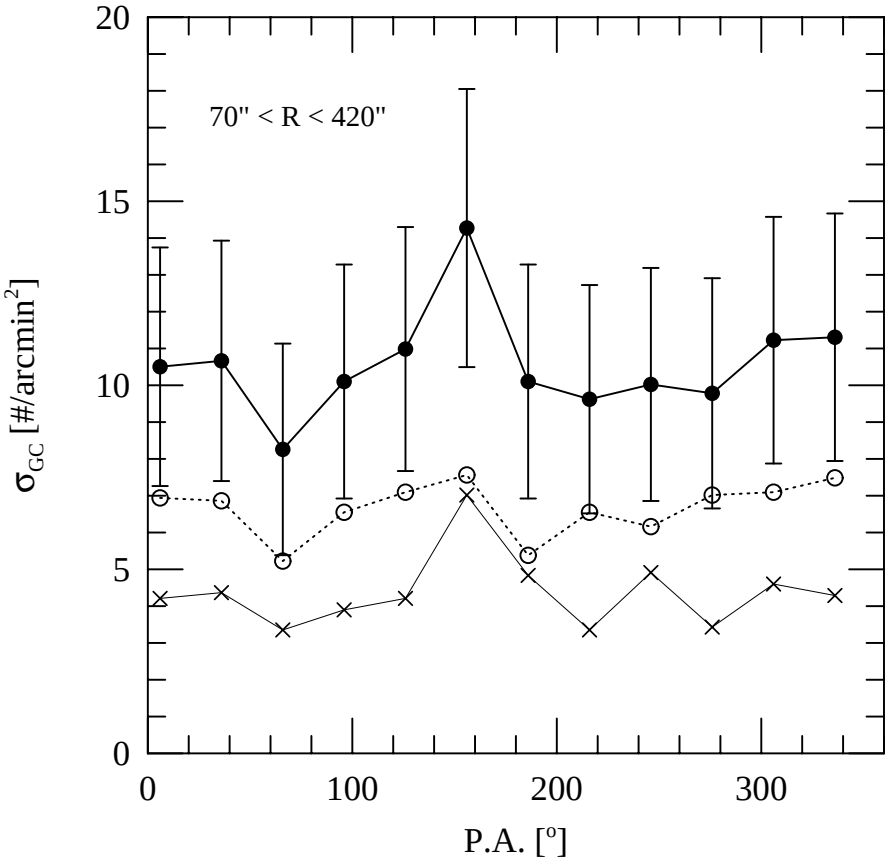

Fig. 9.— Azimuthal variations of the surface number density of the globular clusters with $70'' < r < 420''$. The filled circles, open circles and crosses represent, respectively, the entire GCs, the BGCs and the RGCs.